Chinese Chemical Letters 31 (2020) 865–868

Contents lists available at ScienceDirect

Chinese Chemical Letters

journal homepage: www.elsevier.com/locate/cclet

Communication

# Ternary organic solar cells based on polymer donor, polymer acceptor and PCBM components

Feng Liu[a,c], Cheng Li[c], Junyu Li[d], Chao Wang[a,c], Chengyi Xiao[b,*], Yonggang Wu[a,*], Weiwei Li[b,c,**]

[a] College of Chemistry and Environmental Science, Hebei University, Baoding 071002, China
[b] State Key Laboratory of Organic-Inorganic Composites, Beijing University of Chemical Technology, Beijing 100029, China
[c] Beijing National Laboratory for Molecular Sciences, Key Laboratory of Organic Solids, Institute of Chemistry, Chinese Academy of Sciences, Beijing 100190, China
[d] DSM DMSC R&D Solutions, Geleen 6160 MD, the Netherlands

ARTICLE INFO

*Article history:*
Received 11 June 2019
Received in revised form 26 June 2019
Accepted 27 June 2019
Available online 27 June 2019

*Keywords:*
Ternary organic solar cell
Fullerene
Non-fullerene
Bulk-heterojunction
Charge transport

ABSTRACT

In this work, ternary organic solar cells (OSCs) combining a fullerene derivative $PC_{71}BM$ with a non-fullerene acceptor N2200-F blended with a polymer donor PM6 were reported. Compared with the binary systems, the highest power conversion efficiency (PCE) of 8.11% was achieved in ternary solar cells with 30 wt% N2200-F content, mainly due to the improved short-circuit current density ($J_{sc}$) and fill factor (FF). Further studies showed that the improved $J_{sc}$ could attribute to the complementary absorption of the two acceptors and the enhanced FF was originated from the higher hole mobility and the fine-tuned morphology in the ternary system. These results demonstrate that the combination of fullerene and non-fullerene acceptors in ternary organic solar cells is a promising approach to achieve high-performance OSCs.



Since the discovery of bulk-heterojunction organic solar cells (BHJOSCs) [1], the performance of OSCs based on fullerene acceptors had achieved rapid progress together with the emergence of new donor materials and device optimizing methods [2]. Generally, fullerene acceptors have many advantages, such as high electron mobility, appropriate energy levels that match most donor polymers, and isotropic charge transport. Meanwhile, fullerene acceptors suffer from many shortcomings, such as low absorption coefficient in visible region, complex synthesis and purification, and thus high cost. In order to overcome these shortcomings, a large number of non-fullerene acceptors have been developed [3]. Especially after the first fused-ring electron acceptor ITIC was invented [4], the power conversion efficiencies (PCEs) of OSCs based on non-fullerene acceptors have fully transcended those of the fullerene acceptors [5]. As a result, the PCEs of single-junction OSC have already exceeded 16% [6], which lights up the hope of OSCs for large-scale industrial application.

Ternary OSCs is one of the most effective strategies to enhance the photovoltaic performance [7]. Firstly, the additional third component can broaden the absorption spectrum so as to increase short-circuit current density ($J_{sc}$) [8]. Secondly, the third component can also finely tune the blend morphology, which is instrumental in exciton dissociation and charge transport [9]. Besides, unlike tandem OSCs, there are no recombination layers in ternary OSCs, so the device fabrication process is significantly simplified. Therefore, combining fullerene acceptor with non-fullerene acceptor together in ternary OSCs may bring new potential that utilizes the advantage of the two components to promote the performance.

We are particularly interested in the design, synthesis and application of non-fullerene acceptors based on naphthalene diimides (NDI) and perylene bisimides (PBI) [10]. For example, a PBI dimer-based conjugated polymer was found to provide better photocurrent than that of single PBI-based polymer [10f]. Recently, single-component OSCs based on double-cable conjugated polymers with PBI side chains have achieved great success [11]. Inspired by our previous work, herein, we report our study on ternary OSCs based on these materials. We envisaged that joining

* Corresponding authors.
** Corresponding author at: State Key Laboratory of Organic-Inorganic Composites, Beijing University of Chemical Technology, Beijing 100029, China.
*E-mail addresses:* xiaocy@mail.buct.edu.cn (C. Xiao), wuyonggang@hbu.edu.cn (Y. Wu), liweiwei@iccas.ac.cn (W. Li).

https://doi.org/10.1016/j.cclet.2019.06.051
1001-8417/

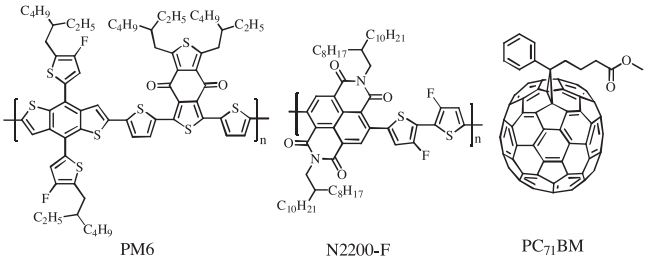


**Fig. 1.** The chemical structures of the polymer donor PM6, polymer acceptor N2200-F and fullerene derivative $PC_{71}BM$.

[6,6]-phenyl-$C_{71}$-butyric acid methyl ester ($PC_{71}BM$) and NDI-based acceptor N2200-F together may not only extend the absorption spectra, but also provide optimized morphology. As a result, the highest PCE of 8.11% was achieved in ternary solar cells with 30 wt% N2200-F content.

The chemical structures of PM6, N2200-F and $PC_{71}BM$ are shown in Fig. 1. PM6 and N2200-F were prepared according to the literatures [12], and the synthetic procedures were also summarized in the Supporting information. The absorption of PM6 covers the entire visible region from 300 nm to 700 nm, with relatively low extinction coefficient in 300–500 nm. On the contrary, N2200-F and $PC_{71}BM$ have strong absorption in 300–500 nm. Besides, the absorption of N2200-F also extends to 800 nm. As can be seen from Fig. 2a and Fig. S1 (Supporting information), the absorption spectra of these three components show an excellent complement covering almost the whole UV-vis-NIR region, which is favorable for light harvesting and producing high photocurrent.

The molecular weight, optical properties and energy levels of PM6, N2200-F and $PC_{71}BM$ are given in Table 1 and Fig. S2 (Supporting information). Both PM6 and N2200-F exhibit moderate molecular weight with $M_n$ of 64.7 kDa and 69.8 kDa. And both PM6 and N2200-F display excellent solubility in common organic solvents, such as chloroform and chlorobenzene, ensuring the solution processing for devices. The energy levels for these three materials are shown in Fig. 2b. Both the lowest unoccupied molecular orbital (LUMO) of N2200-F (-3.9 eV) and the highest occupied molecular orbital (HOMO) of N2200-F (-5.8 eV) lie in between these of PM6 and $PC_{71}BM$, which is conducive to the cascade charge transfer in the ternary solar cells.

The ternary solar cells based on PM6, N2200-F and $PC_{71}BM$ were fabricated with an inverted device structure of ITO/ZnO PM6:N2200-F:$PC_{71}BM$/$MoO_3$/Ag. The ratio of donor/acceptor (Tables S1 and S2 in Supporting information) and the annealing temperature were carefully optimized. It was found that the binary solar cells show optimum donor/acceptor ratio of 1:1 and annealing temperature of 130 °C with active layer thickness of 70–80 nm. Thus, in ternary solar cells, the ratio of donor/acceptor was maintained at 1:1. The optimized results of these ternary cells with different N2200-F content were shown in Table 2 and Table S3 (Supporting information). The optimal *J-V* characteristic was present in Fig. 3. The binary cells based on PM6 and N2200-F achieved the best PCE of 7.34% with open-circuit voltage ($V_{oc}$) of 0.89 V, $J_{sc}$ of 12.26 mA/cm$^2$ and fill factor (FF) of 0.67. Binary solar cells based on PM6 and $PC_{71}BM$ obtained the similar best PCE of 7.38% with higher $V_{oc}$ of 0.92 V, $J_{sc}$ of 12.59 mA/cm$^2$ and FF of 0.63. Solar cells fabricated with PM6:N2200-F:$PC_{71}BM$ ternary blend show higher performance. The champion PCE of ternary cells was 8.11% with 30 wt% N2200-F content, due to the improved $J_{sc}$ of 13.01 and FF of 0.69. As show in the external quantum efficiencies (EQEs) in Fig. 3b, the improved $J_{sc}$ is mainly attributed to the complementary absorption of the two acceptors.

The crystalline properties of pure PM6, N2200-F and their binary and ternary blend films were investigated by two-dimensional grazing-incidence wide-angle X-ray scattering (GIWAXS). Fig. 4 and Fig. S3 (Supporting information) present their diffraction patterns and corresponding out-of-plane (OOP) and in-plane (IP) cuts. Both PM6 and N2200-F show typical $\pi-\pi$ stacking diffraction in the out-of-plane direction, indicating their preferential face-on orientation (Figs. S3a and b). Multiple diffraction peaks can be found in the in-plane direction of both PM6 and N2200-F film, which is attributed to the lamellae packing of polymer main chain. In ternary films, the (100) diffraction peak and (010) diffractions peaks at the OOP direction can be simultaneously observed, indicating mixed orientation. In addition, the ternary blends also displayed the halo diffraction peaks near (010) peaks that could contributed to the $PC_{71}BM$ (Fig. 3b).

**Table 1**
Molecular weight and optical properties of PM6, N2200-F and $PC_{71}BM$.

| Item | $M_n$[a] (kDa) | $M_w$[a] (kDa) | $Đ_M$ | LUMO (eV) | HOMO (eV) |
|---|---|---|---|---|---|
| PM6 | 64.7 | 82.6 | 1.3 | −3.6[b] | −5.5[b] |
| N2200-F | 69.8 | 120.2 | 1.7 | −3.9[c] | −5.8[c] |
| $PC_{71}BM$ | – | – | – | −4.0 | −6.0 |

[a] Determined with GPC at 140 °C using *o*-DCB as the eluent.
[b] Reference [12a].
[c] Reference [12b].

**Table 2**
Characteristics of cells fabricated from chlorobenzene (CB)/diphenyl ether (DPE) (1.0%, v:v) solution with different content of acceptor and annealing at 130 °C. The thicknesses of the active layers are around 70–80 nm.

| PM6:N2200-F:$PC_{71}BM$ | $J_{sc}$ (mA/cm$^2$) | $V_{oc}$ (V) | FF | PCE (%) |
|---|---|---|---|---|
| 1:1:0 | 12.26 | 0.89 | 0.67 | 7.34 |
| 1:0.3:0.7 | 13.01 | 0.91 | 0.69 | 8.11 |
| 1:0:1 | 12.59 | 0.92 | 0.63 | 7.38 |

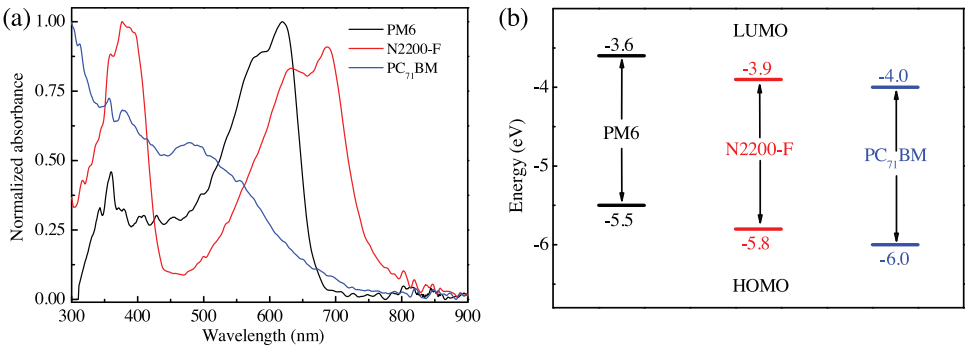


**Fig. 2.** (a) Normalized optical absorption spectra of PM6, N2200-F and $PC_{71}BM$ in thin films. (b) The energy levels of PM6, N2200-F and $PC_{71}BM$.

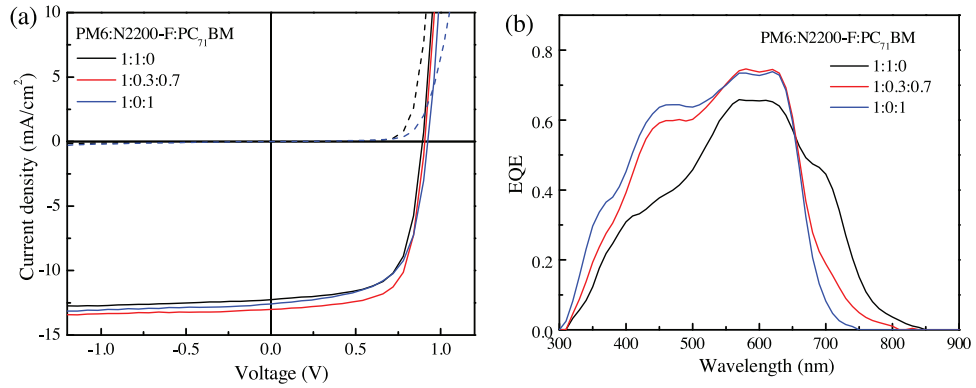


**Fig. 3.** (a) *J-V* curves in dark (dashed line) and under white light illumination (solid line). (b) EQE characteristics of the same devices.

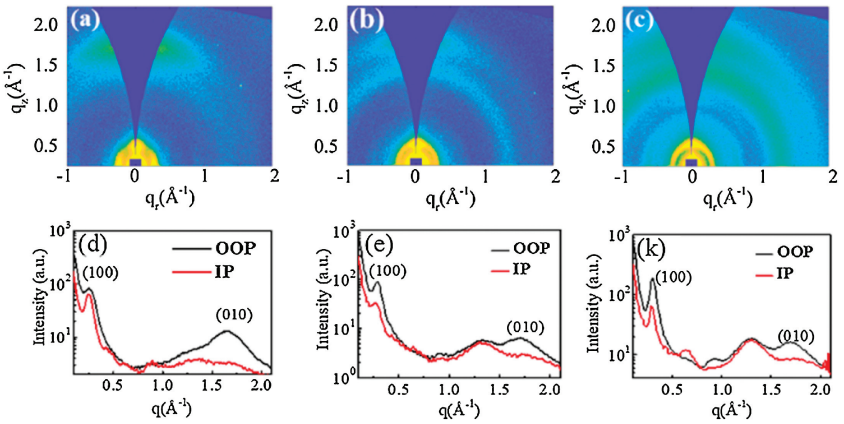


**Fig. 4.** GIWAXS patterns and the corresponding out-of-plane (OOP) and in-plane (IP) cuts. (a, d) PM6:N2200-F:$PC_{71}BM$ = 1:1:0; (b, e) PM6:N2200-F:$PC_{71}BM$ = 1:0.3:0.7; (c, f) PM6:N2200-F:$PC_{71}BM$ = 1:0:1.

These results indicated that the morphology in binary films was inherited in ternary films, resulting in muti-channels for electron transport in N2200-F and $PC_{71}BM$. This could explain the high photocurrent and FF in ternary solar cells.

The surface morphology of the binary and ternary blend films was analyzed by atomic force microscopy (AFM) measurements. Fig. 5 and Fig. S4 (Supporting information) show the height and phase images. The PM6:N2200-F binary system displayed obvious fibrous structures with small root-mean-square (RMS) roughness values. While in the PM6:$PC_{71}BM$ binary system, there is large-sized granular crystals with rough surface, due to the high crystallinity of $PC_{71}BM$. The ternary blend films show compromise surface morphology between the two binary systems. This demonstrates that the morphology of the ternary solar cells can be flexibly regulated by the content of the third component.

Space-charge limited current (SCLC) measurement was used to further investigate the charge transport properties. The detailed *J-V* curves and mobility values are presented in Fig. 6. PM6:N2200-F and PM6:$PC_{71}BM$ binary system show relatively low charge

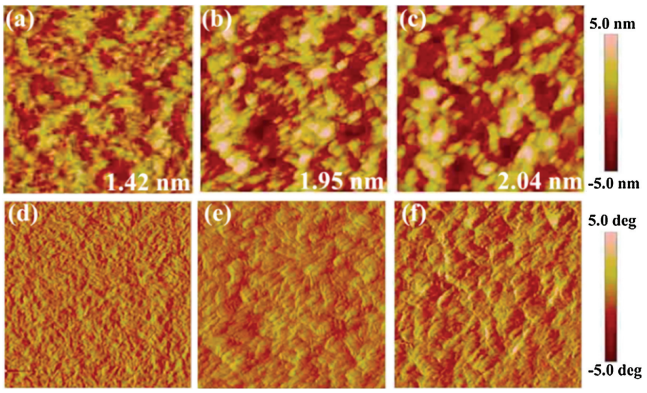


**Fig. 5.** AFM height (a–c) and phase (d–f) images of the optimized solar cells (1 μm × 1 μm). (a, d) PM6:N2200-F:$PC_{71}BM$ = 1:1:0; (b, e) PM6:N2200-F:$PC_{71}BM$ = 1:0.3:0.7; (c, f) PM6:N2200-F:$PC_{71}BM$ = 1:0:1. RMS roughness is also included.

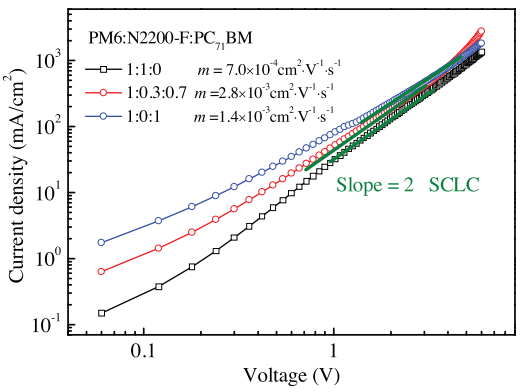


**Fig. 6.** Hole mobilities exacted from SCLC measurements.

transport properties with hole mobilities of $7.0 \times 10^{-4}$ $cm^2$ $V^{-1}$ $s^{-1}$ and $1.4 \times 10^{-3}$ $cm^2$ $V^{-1}$ $s^{-1}$ respectively. While the ternary blend films with 30 wt% N2200-F content show the highest hole mobility of $2.8 \times 10^{-3}$ $cm^2$ $V^{-1}$ $s^{-1}$. These results are consistent with the photovoltaic measurements, which also prove that 30 wt% N2200-F content could finely tune the morphology of the ternary solar cells and facilitate the charge transport.

In conclusion, ternary OSCs combining fullerene acceptor $PC_{71}BM$ with non-fullerene acceptor N2200-F blended with a polymer donor PM6 have been reported in this work. The addition of the third component could not only widen the range of utilizing solar energy, but also regulate the morphology, and thus promote charge transport properties. The high efficiency of 8.11% could be achieved with 30 wt% N2200-F content. These results indicate that combining fullerene acceptor with non-fullerene in ternary OSCs is a feasible way for high-efficient OSCs.

## Acknowledgments

This study is jointly supported by Ministry of Science and Technology of the People's Republic of China (MOST, Nos. 2018YFA0208504, 2017YFA0204702) and the National Natural Science Foundation of China (NSFC, Nos. 51773207, 21574138, 51603209, 91633301). This work was further supported by the Strategic Priority Research Program (No. XDB12030200) of the Chinese Academy of Sciences, Fundamental Research Funds for the Central Universities (No. XK1802-2) and Open Research Fund of State Key Laboratory of Polymer Physics and Chemistry, Changchun Institute of Applied Chemistry, CAS.

## Appendix A. Supplementary data

Supplementary material related to this article can be found, in the online version, at doi:https://doi.org/10.1016/j.cclet.2019.06.051.

## References

[1] G. Yu, J. Gao, J.C. Hummelen, F. Wudl, A.J. Heeger, Science 270 (1995) 1789–1791.
[2] (a) J.K. Lee, W.L. Ma, A.J. Heeger, et al., J. Am. Chem. Soc. 130 (2008) 3619–3623;
(b) J.B. Zhao, W. Ma, H. Yan, et al., Nat. Energy 1 (2016) 15027;
(c) L.T. Dou, Y.S. Liu, Z.R. Hong, G. Li, Y. Yang, Chem. Rev. 115 (2015) 12633–12665;
(d) Y.F. Li, Acc. Chem. Res. 45 (2012) 723–733;
(e) L.Y. Lu, T.Y. Zheng, L.P. Yu, et al., Chem. Rev. 115 (2015) 12666–12731;
(f) H.F. Yao, L. Ye, J.H. Hou, et al., Chem. Rev. 116 (2016) 7397–7457;
(g) J.S. Song, Z.S. Bo, Sci. China Chem. 62 (2019) 9–13.
[3] G.Y. Zhang, J.B. Zhao, H. Yan, et al., Chem. Rev. 118 (2018) 3447–3507.
[4] Y.Z. Lin, J.Y. Wang, X.W. Zhan, et al., Adv. Mater. 27 (2015) 1170–1174.
[5] (a) C.Q. Yan, S. Barlow, X.W. Zhan, et al., Nat. Rev. Mater. 3 (2018) 18003;
(b) J.Q. Zhang, H.S. Tan, X.G. Guo, A. Facchetti, H. Yan, Nat. Energy 3 (2018) 720–731;
(c) J. Yuan, Y.Q. Zhang, Y.P. Zou, et al., Joule 3 (2019) 1140–1151.
[6] (a) Y. Cui, H.F. Yao, J.Q. Zhang, et al., Nat. Commun. 10 (2019) 2515;
(b) X.P. Xu, W. Ma, Q. Peng, et al., Adv. Mater. (2019) 1901872.
[7] (a) Q.S. An, F.J. Zhang, B. Hu, et al., Energy Environ. Sci. 9 (2016) 281–322;
(b) Z.J. Li, W. Zhang, Q. Peng, et al., J. Mater. Chem. C: Mater. Opt. Electron. Devices 6 (2018) 9119–9129;
(c) X.P. Xu, W. Ma, Q. Peng, et al., Adv. Mater. 29 (2017) 1704271;
(d) C.P. Chen, Y.Y. Tsai, Y.C. Chen, Y.H. Li, Sol. Energy 176 (2018) 170–177.
[8] (a) J.Q. Mai, T.K. Lau, X.H. Lu, et al., Chem. Mater. 28 (2016) 6186–6195;
(b) L. Zhong, H.J. Bin, Y.F. Li, et al., J. Mater. Chem. A Mater. Energy Sustain. 6 (2018) 24814–24822.
[9] (a) T. Zhang, X.L. Zhao, D.L. Yang, Y.M. Tian, X.N. Yang, Adv. Energy Mater. 8 (2018) 1701691;
(b) Z.C. Zhou, F. Liu, X.Z. Zhu, et al., Nat. Energy 3 (2018) 952–959.
[10] (a) Y.T. Guo, A.D. Zhang, C. Li, W.W. Li, D.B. Zhu, Chin. Chem. Lett. 29 (2018) 371–373;
(b) C.S. Yu, C. Li, W.W. Li, et al., Chin. Chem. Lett. 29 (2018) 325–327;
(c) C.S. Yu, J.Y. Li, W.W. Li, Chin. J. Chem. 36 (2018) 515–518;
(d) S.C. Zhou, Y.G. Wu, W.W. Li, et al., Acta Phys. Chim. Sin. 34 (2018) 344–347;
(e) Y. Li, Y.H. Xu, W.W. Li, et al., Chin. Chem. Lett. 30 (2019) 222–224;
(f) F. Yang, C. Li, W.W. Li, et al., Chin. J. Polym. Sci. 35 (2017) 239–248.
[11] (a) W.B. Lai, C. Li, W.W. Li, et al., Chem. Mater. 29 (2017) 7073–7077;
(b) G.T. Feng, J.Y. Li, W.W. Li, et al., J. Am. Chem. Soc. 139 (2017) 18647–18656;
(c) G.T. Feng, J.Y. Li, Y.K. He, et al., Joule 3 (2019) 1765–1781.
[12] (a) S.Q. Zhang, Y.P. Qin, J. Zhu, J.H. Hou, Adv. Mater. 30 (2018) 1800868;
(b) J.W. Jung, J.W. Jo, A.K.Y. Jen, et al., Adv. Mater. 27 (2015) 3310–3317.